

Nanoindentation studies of high-temperature oxidized Zircaloy-4 with and without hydrogen

Masato Ito, Hiroaki Muta*, Daigo Setoyama,
Masayoshi Uno, Shinsuke Yamanaka

*Division of Sustainable Energy and Environmental Engineering,
Graduate School of Engineering, Osaka University, 2-1 Yamada-oka, Suita, Osaka 565-0871, Japan*

Received 25 September 2006; received in revised form 13 February 2007; accepted 14 February 2007
Available online 20 February 2007

Abstract

The nanoindentation tests on high-temperature oxidized fuel claddings with/without hydrogenation were performed in order to verify the influence of hydrogen on mechanical behavior of the cladding under a loss of coolant accident (LOCA) condition. Hydrogenated and non-hydrogenated Zircaloy-4 cladding tubes were oxidized in steam at the temperature of 1373–1393 K followed by quenching. The nanoindentation test was performed in the area of inhomogeneous structure called as the Widmann–Stätten structure, composed of the needle-like α' -zirconium grains (α' phase) and the matrix (α phase). The mechanical properties viz. hardness and elastic modulus were evaluated for α' phase and matrix α phase, separately. The hardness and elastic modulus of α' phase are much higher than those of the matrix α phase due to its higher oxygen concentration. There was no significant difference of mechanical properties between the samples with and without hydrogen.

© 2007 Elsevier B.V. All rights reserved.

Keywords: Nuclear reactor materials; Mechanical property; Microstructure; Oxidation; Atomic force microscopy (AFM)

1. Introduction

Zirconium based fuel cladding tube becomes brittle due to rapid β to α transformation and high-temperature oxidation under loss of coolant accident (LOCA) conditions. As expected from the Zr–O phase diagram [1], the β to α rapid transformation by the LOCA creates the Widmann–Stätten structure, composed of the precipitated needle-like α' -zirconium grains (α' phase) and the matrix (α phase). Setoyama and Yamanaka [2] assessed the thermodynamic information of Zr–O–H ternary system using Calculation of Phase Diagram (CALPHAD) technique [3] and showed that hydrogen addition leads to shift ($\alpha + \beta$)/ α phase boundaries towards high oxygen concentration in Zr(H)–O pseudo binary diagram. This calculation results imply that the hydrogen addition leads to increase the oxygen concentration of the precipitated α' phase in the prior- β phase. It has been reported that the solute oxygen leads to decrease the ductility of zirconium alloys [4–6]. Therefore, it would appear

that the hydrogen deteriorates the strength of cladding under LOCA condition by the increase in the oxygen concentration of α' phase. In fact, there are several studies report that hydrogen absorption deteriorates the ductility of the cladding under LOCA [7–9]. Hence, it is important to study the influence of hydrogen on the mechanical properties of the α' phase and the matrix separately in the high-temperature oxidized cladding material.

In order to measure the mechanical properties of the α and α' regions separately, the nanoindentation technique is used. The nanoindentation technique [10–14] has been developed in the past several decades, and the mechanical properties within a few sub-micrometers have been widely discussed. The technique is useful for measuring the mechanical properties of thin films or local structure of various materials with inhomogeneous structures. However, there is limited previous work of applying the nanoindentation technique to evaluate the mechanical properties of nuclear materials. The micro-scale mechanical properties of the oxide film, α -Zr layer and prior- β phase in oxidized zirconium, prepared near the α/β transformation temperature, were studied using nanoindentation technique in our recent study [15]. In the present study, the nanoindentation tests on LOCA simulated Zircaloy-4 with/without hydrogen were performed in the

* Corresponding author. Tel.: +81 6 6879 7905; fax: +81 6 6879 7889.
E-mail address: muta@see.eng.osaka-u.ac.jp (H. Muta).

area of the Widmann–Stätten structure and the hardness and elastic modulus were evaluated for α' phase and α matrix phase separately. The influence of hydrogen on the mechanical properties of each phase was discussed.

2. Experimental procedure

Pressurized Water Reactor (PWR) 17×17 type Zircaloy-4 tubes were used as precursor. The tubes had an internal diameter of 8.22 mm and an external diameter of 9.50 mm. Two types of samples were tested in the present study, one was the as-received alloy and the other was with 500 wt ppm hydrogen added to it. Hydrogenation was carried out using a modified Sieverts' UHV apparatus under a highly pure (7N) hydrogen gas atmosphere. The apparatus is described in detail elsewhere [16]. The samples were oxidized in steam at 1373–1393 K. The cladding specimens were ballooned and ruptured during oxidation, and then quenched. The above-mentioned experimental condition simulates the LOCA condition. The equivalent cladding reacted (ECR) was 20% in both samples. The ECR is defined as the ratio of the converted metal thickness to initial cladding thickness assuming that all the absorbed oxygen converted to stoichiometric zirconia. After the oxidation process, the hydrogen concentration of the samples with and without hydrogen were 25 and 378 wt ppm, respectively.

Afterwards, the broken sections of the claddings were cut, molded in epoxy resin, and the cross sections were polished. The surfaces for all of the samples were treated by a mechano-chemical polishing (CMP) i.e., a mechanical polishing with a chemical treatment using colloidal silica nano-particles. Therefore, neither residual stress nor dislocations remained on the specimen surface. The microstructural data of the sample was obtained by an optical microscope (OLYMPUS BX51M) and the surface roughness was evaluated by an atomic force microscope (AFM, JEOL JSPM-4200).

The nanoindentation was performed for these samples at room temperature in air using the atomic force microscope (JEOL JSPM-4200) with a nano-indenter (TriboScope, Hysitron Inc.). A Berkovich type diamond indenter was used in the present study. The indentation loads were ranging between 500 and 1000 μN , while both the loading and unloading times were chosen to be 5 s.

According to the method of Oliver and Pharr [10], the tip shape of the indenter was calibrated using a reference specimen of fused quartz, and then the indentation load-displacement (P - h) curve was analyzed to calculate the nano-mechanical properties, such as the hardness (H) and reduced modulus (E_r). The hardness [17] and reduced Young's modulus were estimated from the following equations:

$$H = \frac{P_{\max}}{A_C} \quad (1)$$

$$E_r = \frac{1}{2} \sqrt{\frac{\pi}{A_C}} \left. \frac{dP}{dh} \right|_{h=h_{\max}} \quad (2)$$

where A_C stands for the projected contact area at peak load (P_{\max}) of the Berkovich tip, while h_{\max} is the maximum depth.

3. Results and discussion

Fig. 1 shows an optical micrograph of the polished surface of the high-temperature oxidized sample. The figure shows three regions: the oxide film, stabilized α phase, and prior- β phase in the order from outside to inside. The indentation tests were performed at the center of the prior- β phase. The widths of the needle-like α' phase particles in the prior- β phase were to be a few tens of micrometers. The roughness was found to be less than 10 nm from AFM observation. On the contrary, the maximum nanoindentation size i.e., indentation depth and area at the maximum load, was less than 1 μm . Therefore, the impression scale of the nanoindentation, in the present study, was considered to be more than the surface roughness and was remarkably less than the size of the α' phase in the Widmann–Stätten structure.

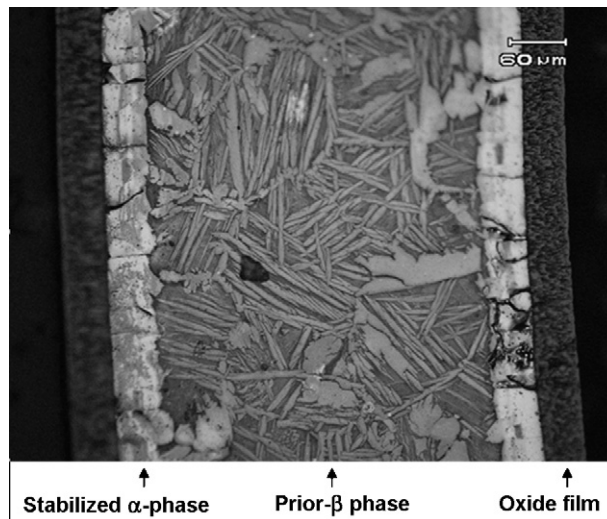


Fig. 1. Metallographic image of the cross section of the oxidized sample.

Fig. 2 shows the hardness profile of the sample with and without hydrogen. Nanoindentation hardness of the prior- β phase in the sample has wave-like character. The wavelength of the hardness modulation in Fig. 2 compares well with the width of the needle-like α' phases in Fig. 1 and it is considered that this modulation reflects the Widmann–Stätten structure. Komatsu et al. [5] revealed that the micro-Vickers hardness increased with increasing oxygen concentration in the prior- β phase. Therefore, since the needle-like precipitated α' phase has higher oxygen content, it is considered that the higher-hardness area corresponds to the α' phase and the lower-hardness area corresponds to the α matrix phase in Fig. 2. Fig. 3 shows the reduced modulus profile of the sample with and without hydrogen. The modulation is also found in the reduced modulus reflecting the Widmann–Stätten structure and its behavior almost consists with that of the hardness.

The obtained hardness values are divided into two groups; one indicates higher values and the other indicates lower values. The average hardness of α' phase and matrix α phase were evaluated from the former group and the latter group, respec-

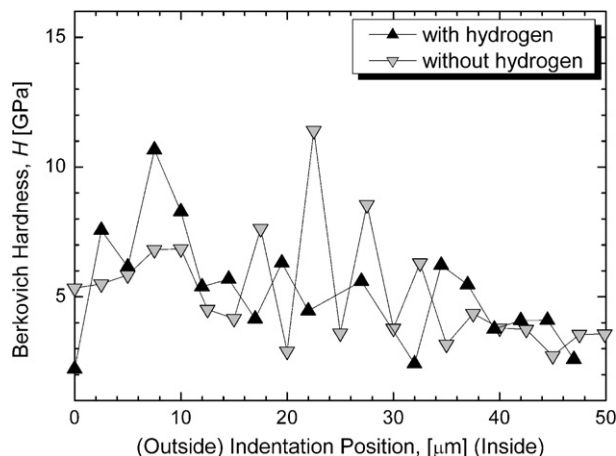


Fig. 2. Profile of the hardness in the Widmann–Stätten structure in samples with and without hydrogen.

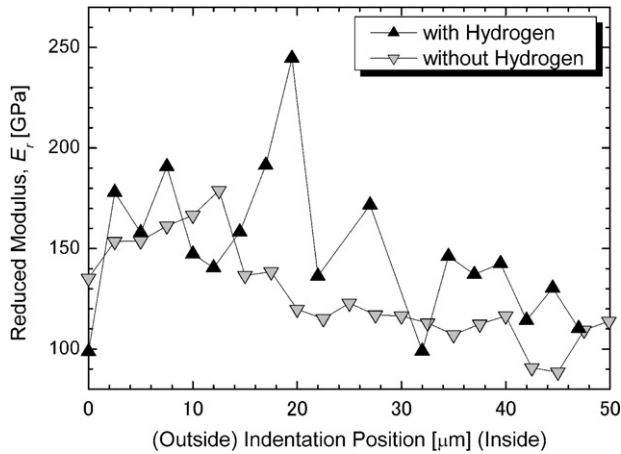


Fig. 3. Profile of the reduced moduli in the Widmann–Stätten structure in samples with and without hydrogen.

tively. Fig. 4 shows the mean hardness of the α' and the matrix α phases with/without hydrogen. Kuroda et al. [18] reported that the Berkovich hardness of pure zirconium with 1000 μN peak load has value of 3.3 GPa. Therefore, the hardness of the matrix α phase is almost equal to the reported value of pure zirconium, which may indicate that the oxygen in the matrix phase is scarce. Additionally, the hardness of α' phase is remarkably higher than that of pure zirconium because of its higher oxygen concentration.

Fig. 5 shows the mean reduced modulus of the α' and the matrix α phases with/without hydrogen. Kuroda et al. [19] and Xu and Shi [20] reported the reduced modulus of pure zirconium as 107 ± 2 and 93.34 ± 5.29 GPa, respectively. Therefore, as in the case of hardness, the elastic modulus of the matrix α phase is nearly the same as the reported values of pure zirconium. The reduced modulus of α' phase is also remarkably higher than that of pure zirconium.

It is found from Figs. 4 and 5 that the variation with hydrogen of mechanical properties for both α' and matrix α phases is within the statistical error. Contrary to the above-mentioned thermodynamic hypothesis that hydrogen addition increases the oxygen concentration of the α' phase in the prior- β phase, influence of hydrogen could not be detected in the present study. It

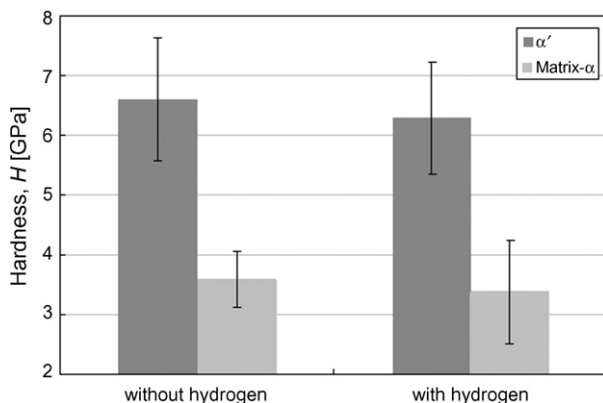


Fig. 4. Mean hardness for the α' and the matrix α phases of samples with and without hydrogen.

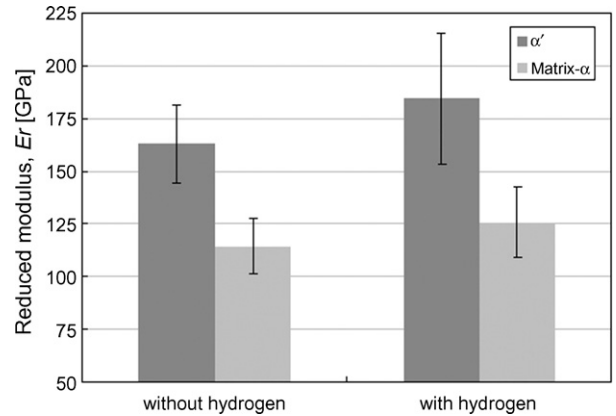


Fig. 5. Mean reduced moduli for the α' and the matrix α phases of samples with and without hydrogen.

may be assumed that the influence of hydrogen is small for the metallic phase and then the degradation of the cladding under LOCA due to hydrogen [7–9] increases with the amount of precipitation of brittle zirconium hydride [21–23]. In the present study, we could not estimate the hardness of hydride precipitate because it is difficult to correlate the morphology of hydride and the nanoindentation hardness in the sample with complex phase. The nanoindentation study for hydrogenated zirconium alloy with simpler phase is under investigation in order to evaluate the properties of hydride precipitate.

4. Conclusion

In the present study, the influence of hydrogen on mechanical behavior of the fuel cladding under a LOCA condition was investigated using nanoindentation technique. The high-temperature oxidized Zircaloy-4 cladding tubes with or without hydrogen were prepared. The nanoindentation test was performed in the center of the Widmann–Stätten structure in the samples, and the mechanical properties viz. hardness and elastic modulus could be evaluated for the needle-like α' -zirconium grains (α' phase) and the matrix (α phase), separately. The mechanical properties of the matrix α phase are almost equal to the pure zirconium, which may indicate that the oxygen in the matrix phase is scarce. The hardness and elastic modulus of α' phase are much higher than those of the matrix α phase due to its higher oxygen concentration. There was no significant difference in mechanical properties between the samples with and without hydrogen.

References

- [1] P. Liang, N. Dupin, S.G. Fries, H.J. Seifert, I. Ansara, H.L. Lukas, F. Aldinger, *Z. Metallkd.* 92 (2001) 7.
- [2] D. Setoyama, S. Yamanaka, *J. Alloys Compd.* 370 (2004) 144.
- [3] N. Saunders, A.P. Miodownik, *CALPHAD (Calculation of Phase Diagrams): A Comprehensive Guide*, Pergamon Press, New York, 1998.
- [4] R.E. Pawel, *J. Nucl. Mater.* 50 (1974) 247.
- [5] K. Komatsu, Y. Takada, M. Mizuta, S. Takahashi, CSNI Report No. 13, 1976.
- [6] A. Sawatzky, *ASTM STP* 681 (1979) 479.

- [7] F. Nagase, T. Fuketa, *J. Nucl. Sci. Tech.* 41 (2004) 723.
- [8] F. Nagase, T. Fuketa, *J. Nucl. Sci. Tech.* 42 (2005) 209.
- [9] J.H. Kim, B.K. Choi, J.H. Baek, Y.H. Jeong, *Nucl. Eng. Des.* 236 (2006) 2386.
- [10] W.C. Oliver, G.M. Pharr, *J. Mater. Res.* 7 (1992) 1564.
- [11] M. Nishibori, K. Kinoshita, *Thin Solid Films* 48 (1978) 325.
- [12] D. Newey, M.A. Wilkins, H.M. Pollock, *J. Phys. E: Sci. Instrum.* 15 (1982) 119.
- [13] J.B. Pethica, in: V. Ashworth, W. Grant, R. Procter (Eds.), *Ion Implantation into Metals*, Pergamon Press, Oxford, 1982, p. 147.
- [14] J.B. Pethica, R. Hutchings, W.C. Oliver, *Phil. Mag.* A48 (1983) 593.
- [15] M. Okui, M. Uno, K. Kurosaki, S. Yamanaka, *J. Alloys Compd.* 363 (2004) 258.
- [16] S. Yamanaka, T. Tanaka, M. Miyake, *J. Nucl. Mater.* 167 (1989) 231.
- [17] B. Bhushan (Ed.), *Handbook of Micro/Nano Tribology*, CRC Press, Boca Raton, FL, 1999, p. 462.
- [18] M. Kuroda, D. Setoyama, M. Uno, S. Yamanaka, *J. Alloys Compd.* 368 (2004) 211.
- [19] M. Kuroda, D. Setoyama, K. Kurosaki, M. Uno, S. Yamanaka, *Spring Mtg. At. Energy Soc. Jpn.*, Kobe, April 28, 2002.
- [20] J. Xu, S.Q. Shi, *J. Nucl. Mater.* 327 (2004) 165.
- [21] M. Kuroda, S. Yamanaka, D. Setoyama, M. Uno, K. Takeda, H. Anada, F. Nagase, H. Uetsuka, *J. Alloys Compd.* 330-332 (2002) 404.
- [22] K.W. Lee, S.I. Hong, *J. Alloys Compd.* 346 (2002) 302.
- [23] U.K. Viswanathan, R.N. Singh, C.B. Basak, S. Anantharaman, K.C. Sahoo, *J. Nucl. Mater.* 350 (2006) 310.